

# FtsEX is required for CwlO peptidoglycan hydrolase activity during cell wall elongation in *Bacillus subtilis*

Jeffrey Meisner,<sup>1</sup> Paula Montero Llopis,<sup>1</sup>  
Lok-To Sham,<sup>1</sup> Ethan Garner,<sup>1†</sup>  
Thomas G. Bernhardt<sup>1\*\*</sup> and David Z. Rudner<sup>1\*</sup>  
*Department of Microbiology and Immunobiology,  
Harvard Medical School, 77 Avenue Louis Pasteur,  
Boston, MA 02115, USA.*

## Summary

The peptidoglycan (PG) sacculus, a meshwork of polysaccharide strands cross-linked by short peptides, protects bacterial cells against osmotic lysis. To enlarge this covalently closed macromolecule, PG hydrolases must break peptide cross-links in the meshwork to allow insertion of new glycan strands between the existing ones. In the rod-shaped bacterium *Bacillus subtilis*, cell wall elongation requires two redundant endopeptidases, CwlO and LytE. However, it is not known how these potentially autolytic enzymes are regulated to prevent lethal breaches in the cell wall. Here, we show that the ATP-binding cassette transporter-like FtsEX complex is required for CwlO activity. In *Escherichia coli*, FtsEX is thought to harness ATP hydrolysis to activate unrelated PG hydrolases during cell division. Consistent with this regulatory scheme, *B. subtilis* FtsE mutants that are unable to bind or hydrolyse ATP cannot activate CwlO. Finally, we show that in cells depleted of both CwlO and LytE, the PG synthetic machinery continues moving circumferentially until cell lysis, suggesting that cross-link cleavage is not required for glycan strand polymerization. Overall, our data support a model in which the FtsEX complex is a remarkably flexible regulatory module capable of controlling a diverse set of PG hydrolases during growth and division in different organisms.

## Introduction

Most bacteria surround themselves with a cell wall exoskeleton composed of peptidoglycan (PG). This macromolecule is assembled from glycan strands cross-linked to one another by short peptides to form a three-dimensional meshwork that encapsulates the cytoplasmic membrane, provides cell shape, and protects the cell from osmotic lysis. In rod-shaped bacteria, the polysaccharide strands are thought to be arranged perpendicular to the long axis of the cell, wrapping around the cylinder with peptide cross-bridges linking the glycan 'hoops' together (Gan *et al.*, 2008; Beeby *et al.*, 2013). Bacterial growth is intimately tied to cleavage and expansion of the covalently closed PG meshwork. To enlarge this matrix, bonds connecting the glycan strands must be broken to incorporate new strands between the existing ones (Weidel and Pelzer, 1964). PG hydrolases play a central role in this process, but their activities must be tightly regulated to prevent excessive degradation of the cell wall and the generation of lethal breaches in this protective layer. The specific enzymes that are responsible for enlarging the cell wall during growth in *Escherichia coli* and *Bacillus subtilis* have recently been identified (Bisicchia *et al.*, 2007; Hashimoto *et al.*, 2012; Singh *et al.*, 2012). However, the mechanisms by which they are regulated have remained mysterious. An understanding of these regulatory systems is likely to reveal new ways to subvert PG biogenesis for therapeutic intervention.

Much has been learned about PG hydrolase regulation in recent years from studies of cell division in the Gram-negative model organism *E. coli*. During cytokinesis, new cell wall is synthesized in the wake of the constricting inner membrane (Burdett and Murray, 1974a,b; Olijhoek *et al.*, 1982). This new septal PG material is initially shared between the developing daughter cells and must be split shortly after it is made to allow outer membrane constriction to closely follow that of the inner membrane (Vollmer *et al.*, 2008). Septal PG splitting is mediated by three PG amidases (AmiA, AmiB, and AmiC) (Heidrich *et al.*, 2002; Priyadarshini *et al.*, 2007), which are in turn regulated by two LytM-domain-containing proteins (EnvC and NlpD) at the cytokinetic ring (Uehara *et al.*, 2010). The LytM domains of these factors lack the catalytic residues normally conserved in LytM-like proteins with PG

Accepted 11 July, 2013. For correspondence. \*E-mail rudner@hms.harvard.edu; Tel. (617) 432 4455; Fax (617) 738 7664. \*\*E-mail thomas@hms.harvard.edu; Tel. (617) 432 6971; Fax (617) 738 7664. †Present address: Department of Molecular and Cellular Biology, Harvard University, 52 Oxford St. Cambridge, MA 02138.

metalloendopeptidase activity. Thus, EnvC and NlpD are thought to be degenerate LytM factors that have lost catalytic activity and instead activate PG hydrolysis by their cognate amidases. AmiA and AmiB are activated by EnvC, while AmiC is activated by NlpD (Uehara *et al.*, 2010). Just as the PG hydrolases must be tightly controlled, their activation by the LytM factors is also likely to be the target of extensive regulation. While the mechanism of NlpD regulation remains unknown, recent studies have revealed that EnvC is regulated by FtsEX, an ATP-binding cassette (ABC) transporter-like complex that forms part of the septal ring division machine (Yang *et al.*, 2011). FtsE is the ATPase and FtsX is the transmembrane domain subunit of the complex. FtsEX recruits EnvC to the septal ring through an interaction between a coiled-coil domain on EnvC and a periplasmic loop of FtsX. Importantly, FtsEX mutants predicted to disrupt ATPase activity still recruit EnvC to the division site but are unable to stimulate amidase activity to promote septal PG splitting. These results suggest that EnvC-dependent activation of cell wall hydrolases at the outer face of the inner membrane is regulated by conformational changes in the FtsEX complex mediated by ATP hydrolysis in the cytoplasm (Yang *et al.*, 2011). A similar pathway appears to function during cell division in the Gram-positive ovococcus *Streptococcus pneumoniae* (Sham *et al.*, 2011). In this case, FtsEX appears to control the activity of PcsB, a factor that shares a similar domain structure with EnvC, possessing an N-terminal coiled-coil domain and a C-terminal PG hydrolase-like domain. However, instead of a LytM domain, the PG hydrolase-like domain of PcsB belongs to the CHAP (cysteine- and histidine-dependent aminohydrolase/peptidase) family (Bateman and Rawlings, 2003). It is currently unclear whether PcsB directly cleaves PG or if, like EnvC, it has lost catalytic activity and functions as an activator of other PG hydrolases.

The results in *E. coli* and *S. pneumoniae* suggest a conserved role for FtsEX in the regulation of PG hydrolase activity during cell division. However, in the rod-shaped Gram-positive organism *B. subtilis*, mutants lacking FtsEX divide normally (Garti-Levi *et al.*, 2008), indicating that the complex is dispensable for division. Here, we implicate *B. subtilis* FtsEX in the control of PG hydrolase activity required for cell elongation. In this organism, two functionally redundant DL-endopeptidases (LytE and CwIO) that cleave peptide cross-bridges are required for cell wall elongation (Bisicchia *et al.*, 2007; Hashimoto *et al.*, 2012). Cells lacking either one of these enzymes are viable, but the inactivation of both is lethal. Depletion of one of these hydrolases in the absence of the other generates short cells that ultimately lyse, indicating that they are critical for expansion of the meshwork during growth. Interestingly, CwIO has a domain organization that resembles that of EnvC and PcsB in that it possesses a coiled-coil domain

preceding its NlpC/P60 DL-endopeptidase domain. We therefore suspected that it might be the target of FtsEX regulation in *B. subtilis*. Here, we show that *B. subtilis* *ftsEX* is indeed in a genetic pathway with *cwIO*. Cells lacking FtsEX and CwIO have indistinguishable phenotypes and both are synthetically lethal with *lytE* mutants. Furthermore, variants of FtsE that are predicted to be ATPase-defective phenocopy loss of function mutations in *ftsE* and *cwIO*. Interestingly, cell surface association of CwIO requires its coiled-coil domain but not FtsX, suggesting that an additional protein functions in this regulatory pathway. Finally, we show that inactivation of CwIO and LytE fails to arrest the directed movement of the cell wall synthetic machinery prior to lysis, consistent with a 'make-before-break' model for PG synthesis in this organism. Overall, our data provide evidence that the FtsEX ABC transporter-like complex is a flexible regulatory module that is employed by different bacteria to control diverse PG hydrolases involved in both cell elongation and division. Another paper in this issue (Dominguez-Cuevas *et al.*, 2013) describes an independent study with similar and complementary results to those described here.

## Results

### *FtsEX is a component of the CwIO peptidoglycan hydrolysis pathway*

LytE and CwIO have similar C-terminal DL-endopeptidase domains but have different N-terminal domains (Ishikawa *et al.*, 1998; Margot *et al.*, 1998; Yamaguchi *et al.*, 2004). LytE contains three LysM domains, a common peptidoglycan-binding motif found in PG hydrolases and other cell surface-associated proteins (Buist *et al.*, 2008). CwIO, on the other hand, has two predicted coiled-coil domains at its N-terminus (Fig. 1A). In both *E. coli* and *S. pneumoniae*, FtsEX is linked to a PG hydrolytic activity through a coiled-coil domain suggesting that CwIO might be similarly connected to FtsEX (Sham *et al.*, 2011; Yang *et al.*, 2011). This led us to examine how many additional PG hydrolases in *B. subtilis* contain coiled-coil domains. Interestingly, CwIO appears to be the only one (data not shown). We further discovered an intriguing genomic association between *ftsEX* and genes encoding coiled-coil-containing PG hydrolases (Fig. 1B). In *E. coli* and most other proteobacteria, *ftsEX* and *envC* homologues are found in different regions of the chromosome. This is also the case for *ftsEX* and *cwIO* in *B. subtilis* and many other *Firmicutes*, including *ftsEX* and *pcsB* in *S. pneumoniae*. However, in epsilon-proteobacteria, like *H. pylori* and *C. jejuni*, an *envC* homologue that encodes a coiled-coil domain fused to a degenerate LytM domain is found immediately downstream of *ftsEX* (Fig. 1B). Moreover, in a subset of *Firmicutes*, a gene encoding a PG hydrolase with a coiled-coil

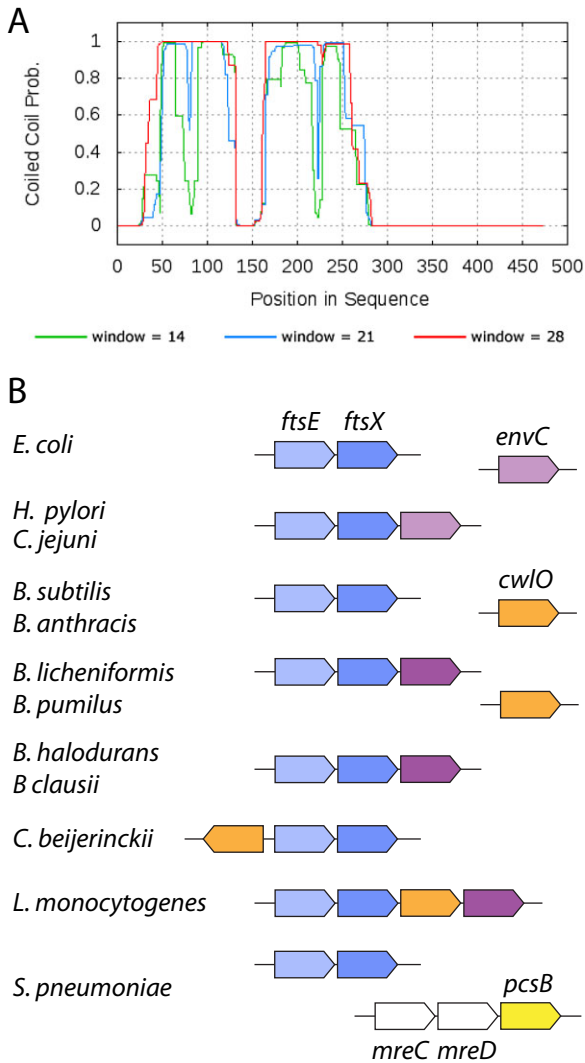


**Fig. 1.** Bioinformatic analysis linking FtsEX and CwIO. A. Coiled-coil prediction for CwIO using COILS (Bioinformatics Toolkit, Max-Planck Institute for Developmental Biology). The predictions were made using 14, 21, and 28 residue windows (shown in green, blue and red respectively). B. Genomic context of *ftsEX* in diverse bacteria. *ftsE* and *ftsX* are coloured light and dark blue respectively. Genes encoding predicted coiled-coil containing LytM proteins with degenerate (e.g. *E. coli envC*) and conserved active site residues are coloured light and dark purple respectively. Genes encoding CwIO homologues with predicted coiled-coil are coloured orange. *pcsB* encoding a CHAPS-domain with a coiled-coil is coloured yellow.

domain is found adjacent to *ftsEX*. In *B. licheniformis* and *B. pumilus*, a gene encoding a coiled-coil-containing LytM with intact catalytic residues lies immediately downstream of *ftsEX*, while *cwIO* is present elsewhere in the genome. A similar genomic organization of *ftsEX* and *lytM* is found in *B. halodurans* and *B. clausii*, however *cwIO* appears to be absent from these bacteria. In *Clostridium beijerinckii*, *cwIO* is immediately upstream of *ftsEX*; in *Listeria monocytogenes*, *ftsEX* is immediately followed by *cwIO* and *lytM* in

tandem (Fig. 1B). Finally, a genetic screen for suppressors of a chemokine that kills *Bacillus anthracis* identified mutations in *ftsX* and a gene that encodes a CwIO homologue (Crawford *et al.*, 2011). Based on this genetic connection, the genomic associations, the predicted coiled-coil domains in CwIO, and the current models for FtsEX function, we hypothesized that FtsEX is a component of the CwIO PG hydrolysis pathway in *B. subtilis*.

To investigate whether FtsEX is necessary for CwIO activity, we took advantage of the synthetic lethality of *lytE* and *cwIO* mutants. If FtsEX is required for CwIO function, then *ftsEX* mutants should also be synthetically lethal with a *lytE* mutant. We constructed a strain containing a *lytE* null mutant and a conditional *lytE* allele under the control of an IPTG-inducible promoter. We then transformed *cwIO* or *ftsEX* deletions into this strain in the presence of IPTG to induce the expression of *lytE*. Both strains grew as well as the parental strain in the presence of inducer. However, when grown in the absence of IPTG, both double mutants suffered a complete loss of viability (Fig. 2A). Similarly, all strains grew equally well in liquid culture in the presence of IPTG, but the strains lacking *ftsEX* and *cwIO* both stopped growing within 60 min after its removal (Fig. 2B). After longer incubation in the absence of IPTG, the cells began to lyse. Immunoblot analysis revealed that CwIO levels were unaffected in the absence of FtsEX (not shown and see below). Finally, an in-frame deletion of *ftsE* and an insertion-deletion of *ftsX* displayed similar synthetic phenotypes with the *lytE* mutant (Fig. 2A), indicating that both the putative ATP binding protein FtsE and its cognate transmembrane protein FtsX are necessary for CwIO function.

To assess the specificity of the *ftsEX-lytE* synthetic lethality, we generated mutants in several DL-endopeptidases and tested them for synthetic phenotypes with an *ftsEX* null mutant. To do so, we constructed a strain with an *ftsEX* deletion and an IPTG-inducible allele of *ftsEX*. We transformed this strain with deletions in *lytE*, *cwIO*, *lytF* or *cwIS*. Only the *lytE* deletion was inviable in the absence of *ftsEX* induction (Fig. 2C). All the other mutants grew indistinguishably from the parental strain. Thus, the synthetic lethality in cells lacking *ftsEX* and *lytE* is specific and not a general feature of DL-endopeptidase mutants.

If *cwIO* and *ftsEX* are in the same genetic pathway as our data suggest, then strains harbouring mutations in *cwIO* and separately in *ftsEX* should have similar phenotypes to each other and to the *cwIO*, *ftsEX* double mutant. It has been reported previously that cells lacking FtsEX are shorter than wild-type (Garti-Levi *et al.*, 2008). Accordingly, we directly compared the cytological phenotypes of *cwIO* and *ftsEX* mutants. The cells were grown in rich medium and analysed by fluorescence microscopy using the membrane dye TMA-DPH. The single *cwIO* and *ftsEX* mutants and the double mutant indeed shared very similar

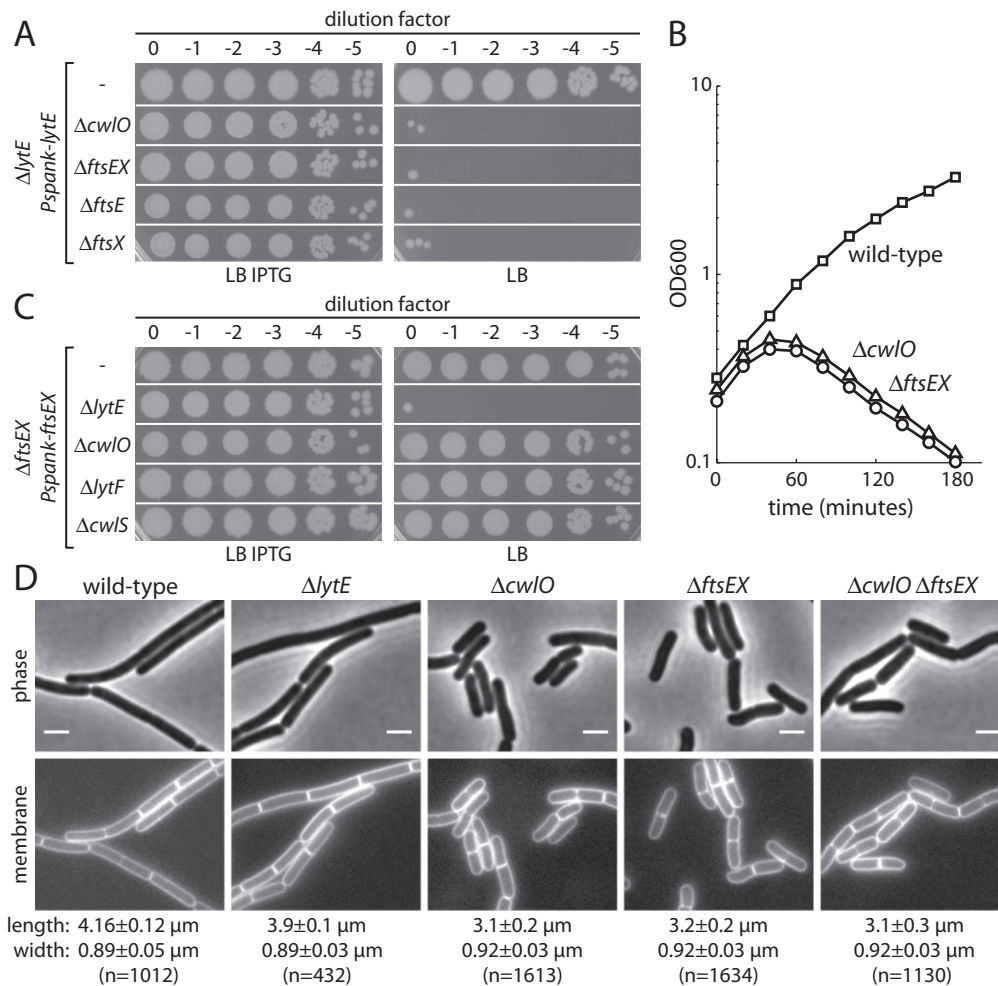


**Fig. 2.** FtsEX and CwIO are in the same PG hydrolysis pathway.

**A.** Synthetic lethality of *ftsEX* and *lytE* mutants. Spot dilutions of the indicated strains in the presence and absence of inducer. Strains were grown in medium supplemented with 1 mM IPTG. Culture densities were normalized, serially diluted 10-fold, and 5  $\mu$ l from each dilution was spotted onto LB agar plates with or without IPTG.

**B.** Cessation of growth following LytE depletion in an *ftsEX* mutant. Parental strain  $\Delta lytE$ ,  $P_{spank-lytE}$  (strain BJM386, squares),  $\Delta cwIO$ ,  $\Delta lytE$ ,  $P_{spank-lytE}$  (strain BJM495, circles), and  $\Delta ftsEX$ ,  $\Delta lytE$ ,  $P_{spank-lytE}$  (strain BJM493, triangles) were grown in CH medium supplemented with 1 mM IPTG at 37°C to mid-exponential phase, washed with medium lacking IPTG and inoculated in CH medium without IPTG (time 0). Cell densities (OD<sub>600</sub>) were monitored every 20 min.

**C.** Specificity of the *ftsEX-lytE* synthetic lethality. Spot dilutions of indicated strains in the presence and absence of inducer as described in (A).

**D.** Cells lacking CwIO, FtsEX, or both have the same cytological phenotypes. Indicated strains were grown in CH medium at 37°C to mid-exponential phase and visualized by phase-contrast (top) and fluorescence (bottom) microscopy using the membrane stain TMA-DPH. Mean cell lengths from 2–3 experiments and standard deviation between experiments as are shown. Scale bar indicates 1  $\mu$ m.

morphological phenotypes. The mutant cells were shorter and wider than wild-type and often slightly bent or curved (Garti-Levi *et al.*, 2008). Moreover, quantitative analysis using cytoplasmic mCherry fluorescence revealed that the single and double mutants were similar to each other in cell length and width (Figs 2D and S1). For comparison, we also analysed cells lacking *lytE*. The *lytE* mutant was virtually indistinguishable from wild-type with respect to cell size and shape, but as reported previously (Ishikawa *et al.*, 1998) had a mild cell separation defect with a slightly higher proportion of cells present in chains

(Figs 2D and S1 and data not shown). Altogether, these results indicate that *cwIO* and *ftsEX* reside in the same genetic pathway, and support the idea that FtsEX is specifically required for the endopeptidase activity of CwIO.

#### *FtsEX* is involved in cell elongation in *B. subtilis*

Classical genetic screens in *E. coli* identified conditional mutants that fail to undergo cell division and form long, filamentous cells (Van De Putte *et al.*, 1964). The mutants were appropriately named *fts* for filamentous temperature-

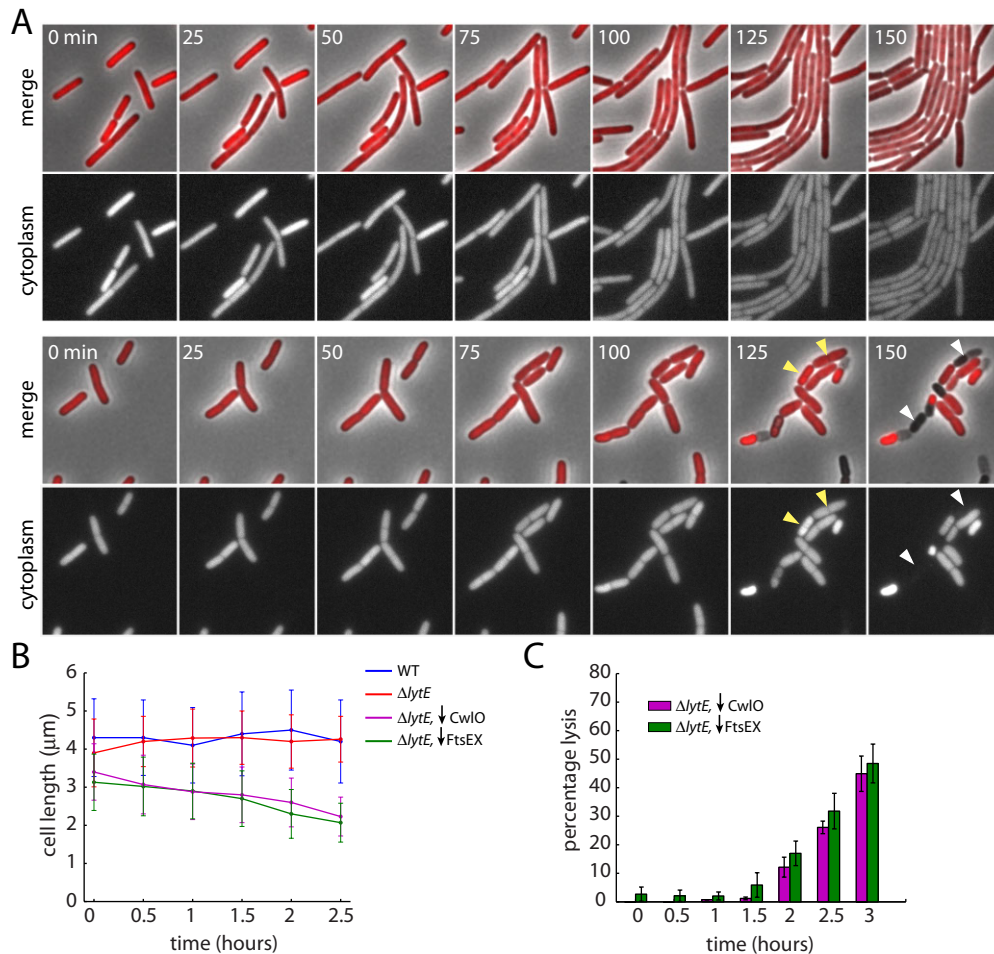


**Fig. 3.** FtsEX is required for cell elongation.

A. Time-lapse fluorescence microscopy of  $\Delta lytE$  (BJM186) (upper) and  $\Delta lytE, \Delta ftsEX, P_{spank-ftsEX}$  (BJM754) (lower). To facilitate quantitative image analysis, both strains harbour *mCherry* expressed under constitutive control to label the cytoplasm. Cells were grown in CH medium supplemented with 1 mM IPTG at 37°C to mid-exponential phase, washed with medium lacking IPTG and inoculated in CH medium. After 1 h of growth in shaking flasks, cells were mounted on agarose pads in a humidified incubator at 32°C and visualized by phase-contrast and fluorescence microscopy every 5 min for 3 h. Merged images of phase-contrast and cytoplasmic *mCherry* (top) and *mCherry* (bottom) are shown. Cell division without significant elongation upon FtsEX depletion is highlighted (yellow caret). Examples of cell lysis are indicated (white caret).

B. Quantitative analysis of cell length during depletion of FtsEX and CwlO. Cytoplasmic *mCherry* images from the time-lapse movies were analysed using MicrobeTracker to assess cell length. More than 400 cells were analysed for each time point. Strains were wild-type (BJM172),  $\Delta lytE$  (BJM186),  $\Delta lytE, \Delta ftsEX, P_{spank-ftsEX}$  (BJM754) and  $\Delta lytE, \Delta cwlO, P_{spank-cwlO}$  (BJM692). Because the cells were grown for 1 h in the absence of inducer before imaging, the strains undergoing depletion of FtsEX and CwlO are already shorter at the first time point.

C. Quantitative analysis of cell lysis during depletion of FtsEX and CwlO in cells lacking *LytE*. Phase-contrast and *mCherry* images from the time-lapse movies were analysed for lysis. More than 400 cells were analysed for each time point.

sensitive. Based on this nomenclature and subsequent studies of FtsEX in *E. coli* (and *S. pneumoniae*), it would be expected that *B. subtilis* FtsEX is also involved in cell division. However, the original description of the *ftsEX* mutant phenotype in *B. subtilis* (Garti-Levi *et al.*, 2008) and the genetic and cytological analysis presented above appear to challenge that expectation. To more clearly discriminate between an involvement in cell elongation and cell division, we monitored the effects of FtsEX depletion in a  $\Delta lytE$  mutant by time-lapse microscopy. To aid in our quantitative analysis of cell length and division, the strain

constitutively expressed *mCherry* to label the cell cytoplasm. The cells were initially grown in rich medium at 37°C in the presence of IPTG to induce expression of FtsEX. Under these conditions, cell growth ceases 120 min after removal of inducer (not shown). Accordingly, the cells were grown in shaking culture for 60 min after removal of IPTG prior to mounting on agarose pads. The cells were then monitored by time-lapse microscopy at 32°C. The parental strain, a *lytE* mutant that contained wild-type *ftsEX*, doubled in cell length and underwent division approximately every 60 min (Fig. 3A upper panels). By contrast,

depletion of FtsEX in cells lacking *lytE*, caused a decrease in cell elongation but did not significantly affect cell division (Fig. 3A lower panels). As a result, the cells shortened during the course of the experiment. Quantitative analysis revealed a steady decrease in average cell length (Fig. 3B). Further incubation in the absence of inducer resulted in cell bulging and bending and ultimately lysis (Fig. 3A and C). Similar results were obtained in a *lytE* mutant in which CwIO was depleted (Figs 3B and C, and S2). These results provide strong evidence that, despite its name, *B. subtilis* FtsEX functions in cell elongation rather than cell division. Furthermore, these results provide additional support for the idea that FtsEX regulates CwIO endopeptidase activity to promote expansion of the PG meshwork along the cell cylinder.

#### *The stress-response transcription factor $\sigma^l$ is required in the absence of the FtsEX*

Devine and co-workers recently provided evidence that the CwIO is the primary DL-endopeptidase in vegetative cells, while LytE becomes important when cells experience envelope stress (Salzberg *et al.*, 2013). This model was based on the observation that *lytE* expression is, in part, controlled by the stress-response sigma factor  $\sigma^l$  (Tseng *et al.*, 2011). Furthermore, a *sigI* deletion was found to be synthetically lethal with a *cwIO* mutant and this lethality could be suppressed by ectopic expression of *lytE* (Salzberg *et al.*, 2013). Our results showing that *ftsEX* is in the same genetic pathway as *cwIO* predict that *ftsEX* and *sigI* should also be a synthetic lethal pair. To test this, we constructed a *sigI* mutant with conditional alleles of *ftsEX* and *cwIO*. As expected, in the presence of IPTG, the strains were indistinguishable from  $\text{SigI}^+$  cells but in the absence of inducer they were both inviable (Fig. 4A). Interestingly, in liquid culture, depletion of CwIO or FtsEX resulted in a more rapid cessation of growth and lysis in the *sigI* mutant than in cells lacking *lytE* (Fig. 4B and data not shown). We interpret this to mean that  $\sigma^l$  controls genes in addition to *lytE* that contribute to cell envelope integrity. These results provide further support for the idea that FtsEX and CwIO function in the same pathway and that this is the primary hydrolytic pathway for cell elongation during vegetative growth.

#### *The FtsEX-CwIO pathway is necessary for efficient entry into sporulation*

Cells lacking FtsEX are delayed in entry into the morphological process of sporulation (Garti-Levi *et al.*, 2008). Specifically, asymmetric cell division is retarded and this can be attributed to a delay in the activation of the master transcriptional regulator Spo0A. Based on its similarity to ABC transporters, FtsEX was proposed to import an envi-

ronmental signal required to trigger timely Spo0A activation. To investigate whether FtsEX has a second unrelated function involved in entry into sporulation or the observed defect was related to its role in regulating PG hydrolysis, we compared sporulating cells lacking *ftsEX* or *cwIO*. Synchronous sporulation was induced by nutrient downshift and polar division was monitored by fluorescence microscopy using the membrane dye TMA-DPH. We observed a similar delay in asymmetric division in the two mutants compared with wild-type and cells lacking LytE (Fig. 4C). Two hours after initiation of sporulation, 38% and 44% ( $n > 1500$ ) of the wild-type and  $\Delta\text{lytE}$  mutants, respectively, had undergone asymmetric division, as compared with 20% and 28% ( $n > 1500$ ) of the  $\Delta\text{cwIO}$  and  $\Delta\text{ftsEX}$  mutant cells. At hour 3, 58% and 61% ( $n > 1500$ ) of wild-type and the  $\Delta\text{lytE}$  mutant cells, respectively, had completed asymmetric division compared with 40% and 52% ( $n > 1500$ ) of the  $\Delta\text{cwIO}$  and  $\Delta\text{ftsEX}$  mutants. Consistent with the idea that FtsEX and CwIO act in the same pathway, a similar delay was observed in the double mutant (not shown). To more precisely assess the timing of Spo0A activation, we monitored a Spo0A-responsive promoter ( $P_{\text{spoIIE}}$ ) fused to *lacZ*. Activation was delayed by approximately 30 min in both  $\Delta\text{ftsEX}$  and  $\Delta\text{cwIO}$  mutants compared with wild-type and the  $\Delta\text{lytE}$  mutant (Fig. 4D). Taken together, these results suggest that the role of FtsEX in promoting efficient entry into sporulation is through its regulation of CwIO.

#### *ATP binding and hydrolysis by FtsE is required for CwIO function*

FtsEX is a member of the ATP-binding cassette (ABC) transporter superfamily. ABC transporters use the chemical energy of ATP hydrolysis to induce conformational changes that promote transport or regulate diverse physiological processes (Higgins, 1992; Rees *et al.*, 2009). These transporters consist of two nucleotide-binding domains (NBD) and two transmembrane domains (TMD). Each domain can exist as a separate protein; NBD and TMD can be joined to make half-transporter proteins; or all four domains can be present in a single polypeptide. The NBD has one set of highly conserved residues that bind ATP and another that catalyse hydrolysis. In the case of FtsEX, FtsE possesses the NBD while FtsX contains four transmembrane segments. Work in *E. coli* and *S. pneumoniae* suggest that FtsEX does not translocate substrates across the membrane but rather is involved in coupling PG hydrolysis to division-associated activities (Arends *et al.*, 2009). Amino acid substitutions in FtsE that are predicted to abrogate nucleotide binding and hydrolysis are unable to stimulate septal PG hydrolysis in *E. coli* (Yang *et al.*, 2011). To investigate whether *B. subtilis* FtsE activity is similarly required for CwIO function, we generated mutants in con-

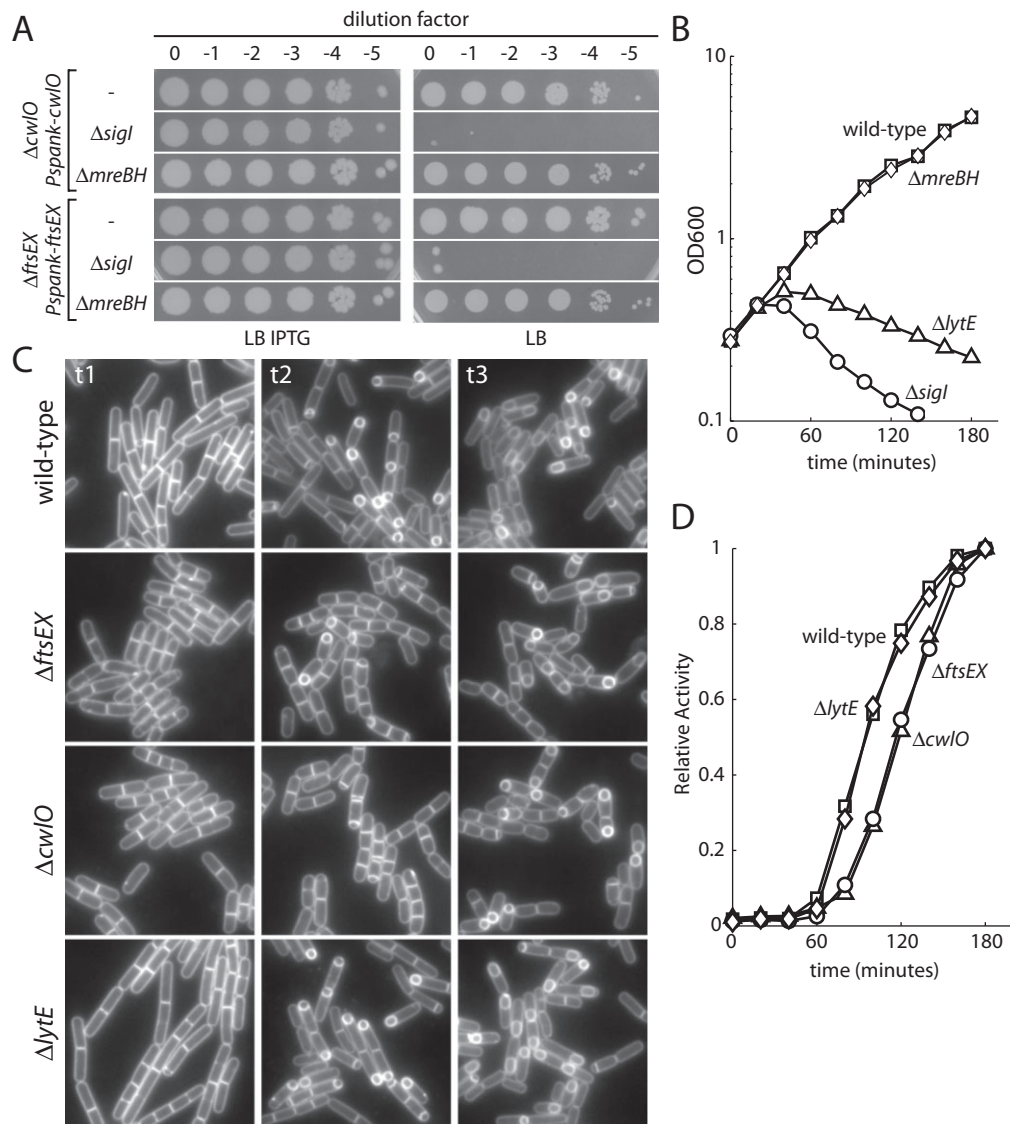


**Fig. 4.** FtsEX and CwIO mutants have indistinguishable phenotypes.

**A.** Synthetic lethality of *ftsEX* and *sigI* mutants. Spot dilutions as described in Fig. 2 of the indicated strains in the presence and absence of inducer.

**B.** Cessation of growth following CwIO depletion in cells lacking, *lytE*, *sigI* and *mreBH*.  $\Delta cwIO$ ,  $P_{spank} cwIO$  (strain BJM433),  $\Delta lytE$ ,  $\Delta cwIO$ ,  $P_{spank} cwIO$  (strain BJM406),  $\Delta sigI$ ,  $\Delta cwIO$ ,  $P_{spank} cwIO$  (strain BJM967) and  $\Delta mreBH$ ,  $\Delta cwIO$ ,  $P_{spank} cwIO$  (strain BJM969) were grown in CH medium supplemented with 1 mM IPTG to mid-exponential phase, washed with medium lacking IPTG and inoculated in CH medium without IPTG (time 0). Cell densities were monitored every 20 min.

**C.** CwIO and FtsEX mutants are delayed in polar division during spore formation. Fluorescent images of cells stained with the membrane dye TMA-DPH at the indicated times after the initiation of sporulation. Strains were wild-type (BJM874),  $\Delta ftsEX$  (BJM900),  $\Delta cwIO$  (BJM902),  $\Delta lytE$  (BJM898).

**D.** Cells lacking CwIO or FtsEX are delayed in the activation of the Spo0A transcription factor. The strains in (C) with a Spo0A-responsive promoter ( $P_{spoII}$ ) fused to *lacZ* were analysed for  $\beta$ -galactosidase activity at the indicated times after resuspension in sporulation medium.

served residues involved in ATP binding (K41) and hydrolysis (D162). In support of the idea that both nucleotide binding and hydrolysis are important for activating CwIO, these mutants failed to complement an *ftsE* deletion and were synthetic lethal with a  $\Delta lytE$  mutant (Fig. 5A). Importantly, the mutant FtsE proteins accumulated to levels within twofold of wild-type (Fig. 5B).

#### Cell surface-association of CwIO depends on its coiled-coil domain but is independent of FtsX

FtsX contains four TM segments with two extracellular loops. The coiled-coil domains of EnvC (*E. coli*) and PcsB (*S. pneumoniae*) have been shown to interact with the first extracellular loop (loop 1) between TM segments one and

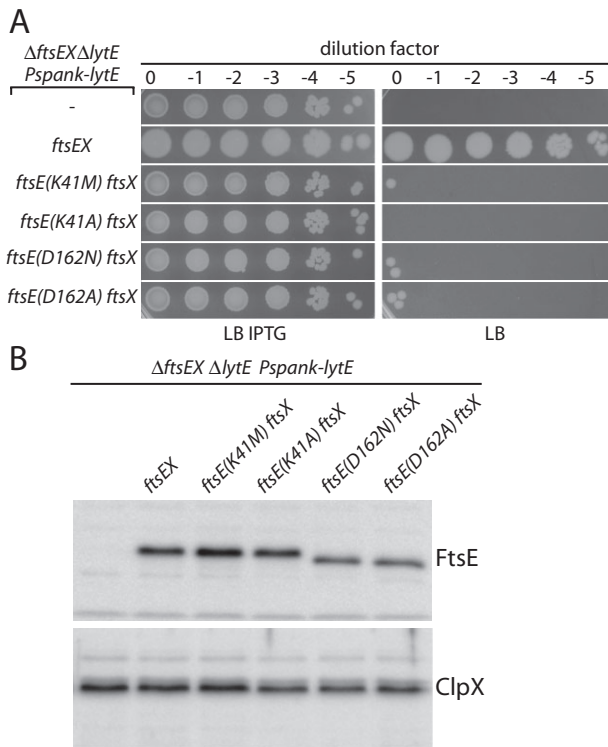


**Fig. 5.** FtsE mutants predicted to disrupt ATP binding and hydrolysis are required for CwIO activity. A. Point mutants in FtsE that are predicted to impair ATP binding and hydrolysis are synthetic lethal with  $\Delta lytE$ . Spot dilutions as described in Fig. 2 in the presence and absence of inducer. Indicated strains harboured a deletion of *ftsEX* at its native locus and a wild-type or mutant copy at an ectopic site (*amyE*). B. Immunoblot analysis of wild type and FtsE mutant proteins. Cytoplasmic ClpX was analysed to control for loading.

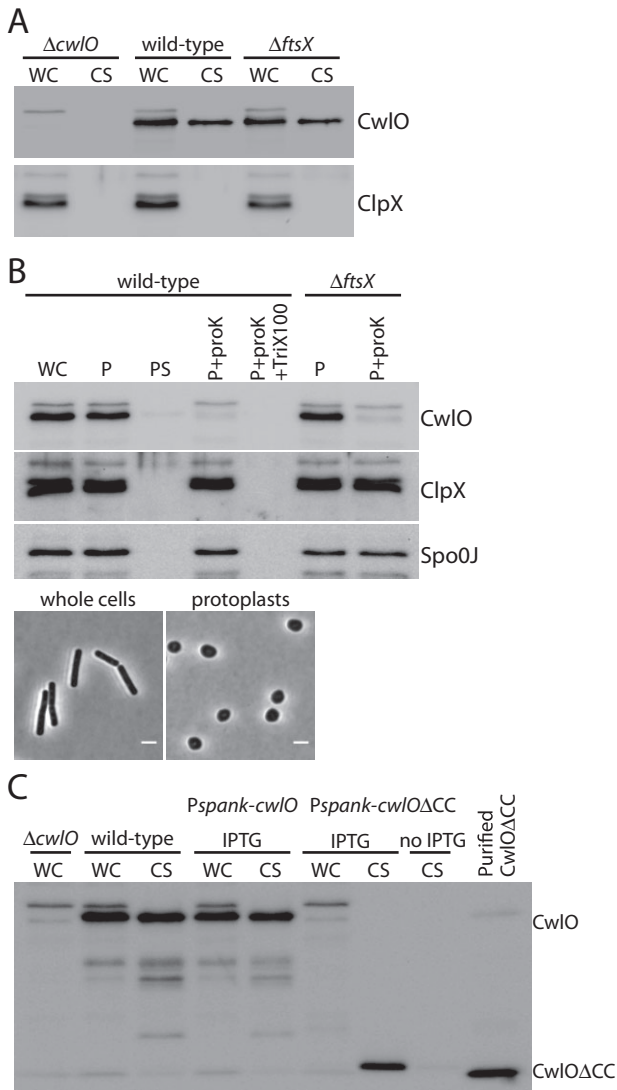
two, and this interaction is important for anchoring EnvC and PcsB to the outer face of the cytoplasmic membrane (Sham *et al.*, 2011; Yang *et al.*, 2011). Accordingly, we wondered whether *B. subtilis* FtsX also promotes the association of CwIO with the cell surface. To investigate this, we monitored the presence of CwIO in whole cell lysates and the culture supernatant. Immunoblot analysis revealed that in wild-type cells approximately 60% of CwIO is cell-associated and 40% is shed into the media (Fig. 6A). Importantly, there was no significant change in the amount of CwIO in the culture supernatant in the presence or absence of FtsX. To rule out the possibility that CwIO remained cell-associated through an interaction with the cell wall rather than at the membrane surface, we degraded the PG with lysozyme in hypertonic buffer generating protoplasts (Fig. 6B). After centrifugation, the presence of CwIO in the supernatant and the protoplast pellet was assessed by immunoblot. All the surface-associated CwIO that was present prior to lysozyme digestion remained associated with the protoplasts and virtually none was present in the supernatant (Fig. 6B). Importantly,

the CwIO associated with the protoplasts was susceptible to proteolysis by proteinase K while two cytoplasmic proteins were not, indicating that CwIO was located on the outside of the cell membrane.

Finally, to determine if surface association of CwIO depends on its coiled-coil domain, we engineered strains that express full-length CwIO and a coiled-coil deletion mutant (CwIO $\Delta$ CC) and monitored the amount of CwIO shed into the cell supernatant. Strikingly, virtually all the CwIO $\Delta$ CC mutant protein was present in the culture medium (Fig. 6C). Taken together, these results indicate that CwIO is retained at the outer surface of the cytoplasmic membrane via an interaction that requires its coiled-coil domain, but that this association does not require FtsX. This observation suggests that an as yet unidentified factor may be interacting with and participating in CwIO regulation in addition to FtsX. Furthermore, the interaction of CwIO with this factor may be required for CwIO to interface with FtsX. Consistent with this proposal, we were unable to detect an interaction between FtsX and purified CwIO in vitro using protein-protein interaction assays with purified full-length FtsX reconstituted into membrane nanodiscs or the soluble extracellular loop 1 (Fig. S3). Furthermore, we failed to detect a significant interaction between loop 1 of FtsX and CwIO in a bacterial two-hybrid assay (not shown).

#### *The cell wall elongation machinery moves in a directed and circumferential manner independently of CwIO and LytE activity*

In *E. coli*, it was recently shown that three functionally redundant DD-endopeptidases that cleave cross-linked stem peptides are required for cell wall elongation. Furthermore, upon their depletion cell wall synthesis ceases (Singh *et al.*, 2012). These observations are consistent with the idea that in *E. coli* synthetic and degradative activities are coupled to growth and suggest that cleavage of the peptide cross-links is a prerequisite for new PG synthesis (Burman and Park, 1984). Gram-positive bacteria, like *B. subtilis*, have a more complex multilayered PG meshwork with synthesis of new cell wall occurring at the membrane surface in an inside-to-outside growth mechanism (Koch and Doyle, 1985). The current view is that synthesis and cross-linking of the new material into the meshwork occurs prior to cleavage of old linkages in a so-called 'make-before-break' mode of synthesis (Koch *et al.*, 1981). We therefore wondered whether or not PG synthesis in *B. subtilis* depends on the elongation endopeptidases CwIO and LytE. To investigate this, we took advantage of our ability to monitor the directed movement of the PG elongation machinery by time-lapse fluorescence microscopy in *B. subtilis* (Garner *et al.*, 2011). We have shown previously that this movement abruptly ceases upon addition of beta-lactams and other cell wall



synthesis inhibitors, suggesting that it is reporting on PG synthesis. To monitor the dynamic movement of the cell wall synthetic complex, we used a GFP fusion to Mbl (GFP-Mbl). Mbl is one of the three filament-forming MreB isoforms in *B. subtilis* that function as a scaffold for the PG synthetic machinery (Jones *et al.*, 2001). We introduced a xylose-inducible *gfp-mbl* fusion at an ectopic locus in a strain lacking both LytE and FtsEX that harboured an IPTG-inducible allele of *ftsEX*. Cells were initially grown in rich medium at 37°C in the presence of IPTG. They were then washed with medium lacking inducer and grown in medium with 10 mM xylose to induce expression of GFP-Mbl. After 2 h of FtsEX depletion, the cells were spotted on an agarose pad and GFP-Mbl was imaged by fluorescence microscopy. GFP-Mbl was also monitored in a control strain lacking LytE. As observed previously, in the control strain GFP-Mbl moved in a directed manner

**Fig. 6.** The CwIO coiled-coil domain is necessary for cell surface association.

A. Surface association of CwIO does not depend on FtsX. Wild-type (BJM001) and strains lacking *cwIO* (BJM054) and *ftsX* (BJM072) were grown in LB medium to mid-exponential phase. Equivalent amounts of whole cell lysate (WC) and cell culture supernatant (CS) (concentrated by trichloroacetic acid precipitation) were separated by SDS-PAGE and CwIO and cytoplasmic ClpX were assessed by immunoblot analysis.

B. Surface association of CwIO in the absence of peptidoglycan cell wall and FtsX. Mid-exponential phase cells (wild-type BJM001 and  $\Delta ftsX$  BJM072) were treated with lysozyme in hypertonic medium to generate protoplasts. Equivalent amounts of whole cell lysates (WC), protoplast lysates (P), and protoplast supernatants (PS) from wild-type and  $\Delta ftsX$  were separated by SDS-PAGE. To determine whether CwIO was located on the outside of the cell, intact protoplasts and protoplasts disrupted with Triton X-100 were treated with proteinase K (P + proK and P + proK+TriX100 respectively). All samples were analysed by immunoblot for CwIO (top), ClpX (middle) and Spo0J (a second cytoplasmic control protein, bottom). Phase-contrast images of cells before and after treatment with lysozyme are shown below.

C. Surface association of CwIO requires its amino-terminal coiled-coil domain. Wild-type (BJM001),  $\Delta cwIO$  (BJM054), and strains lacking *cwIO* harbouring an IPTG-inducible *cwIO* gene (BJM372) or *cwIO* lacking its coiled-coil domain (BJM929) were grown in LB medium supplemented with 1 mM IPTG to mid-exponential phase. Equivalent amounts of whole cell lysates (WC) and cell culture supernatants (CS) were separated by SDS-PAGE and analysed by Western blot with anti-CwIO antiserum. Purified recombinant CwIO lacking its N-terminal coiled-coil (and 40 additional residues) was included as a positive control.

perpendicular to the long axis of the cell (Fig. 7A and Movie S1). This movement is difficult to discern in the still images but it can be seen in the kymographs in Fig. 7 and in the Movie in supplemental material. In cells depleted of FtsEX, there was significant heterogeneity in cell size and shape and in the appearance of the GFP-Mbl foci. However, GFP-Mbl foci moved in a directed, circumferential manner until cell lysis, even in significantly shorter, bulged and bent cells (Fig. 7B and Movies S2–S4). The kymographs in Fig. 7B show two cells one in which the synthetic machinery moves for the entire movie and another in which movement continues until lysis. Notably, we did not observe a cessation of GFP-Mbl movement prior to lysis as was found in strains in which components of the PG synthetic machinery were depleted (e.g. RodA, RodZ, PbpA and PbpH) or upon treatment with antibiotics that inhibit PG synthesis (Garner *et al.*, 2011). Similar results were obtained in strains lacking LytE in which we depleted CwIO (not shown). Collectively, these results indicate that the elongation mode of PG synthesis continues unabated when the two elongation cell wall hydrolases are inactivated until the cells lyse. Thus, our findings are consistent with the idea that PG synthesis can occur even in the absence of the endopeptidases required for cell wall elongation. As such, they favour the make-before-break model of cell wall elongation in *B. subtilis*.

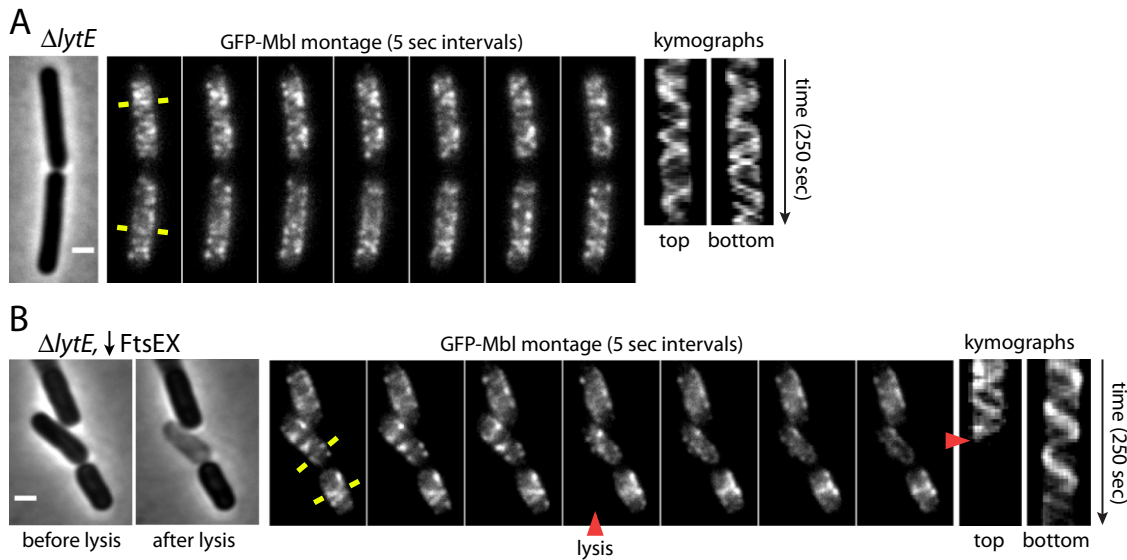


**Fig. 7.** Depletion of PG hydrolase activity does not arrest the cell wall synthetic machinery. Time-lapse images of GFP–Mbl in  $\Delta\text{lytE}$ ,  $P_{\text{xytA}}\text{-gfp-mbl}$  (BJM1007, panel A) and  $\Delta\text{lytE}$ ,  $\Delta\text{ftsEX}$   $P_{\text{spank}}\text{-ftsEX}$ ,  $P_{\text{xytA}}\text{-gfp-mbl}$  (BJM839, panel B). Cells were grown in CH medium supplemented with 1 mM IPTG at 37°C to mid-exponential phase, washed with medium lacking IPTG and inoculated in CH medium. After 120 min of growth in shaking flasks cells were immobilized on agarose pads and then visualized by fluorescence microscopy every 5 s for 250 s at 32°C. Dynamic movement can be seen in the still images or in the kymographs that represent 50 images over 250 s. Representative cells in which GFP–Mbl foci move for the entire movie and an example in which signal is lost at the time of lysis are indicated (red caret). Scale bar indicates 1  $\mu\text{m}$ .

## Discussion

### *FtsEX is a flexible regulatory module for the control of PG hydrolysis*

Growth and division in bacteria involve a highly choreographed interplay between synthesis and degradation of the PG layer. To expand this covalently closed meshwork during growth, hydrolases must cleave peptide cross-links to allow for the synthesis and/or incorporation of new material. The mechanisms responsible for controlling these processing enzymes to prevent the formation of lethal breaches in the wall are only just beginning to be uncovered. In *B. subtilis*, two functionally redundant DL-endopeptidases are the principal enzymes required for cell wall elongation. Here, we provide evidence that one of them, CwIO, is regulated by the FtsEX ABC transporter-like complex. Our results highlight the versatility of this ABC system for regulating diverse families of PG hydrolases during different phases of growth.

By analogy to the proposed role of FtsEX in *E. coli* and *S. pneumoniae* in cytokinesis (Sham *et al.*, 2011; Yang *et al.*, 2011), we envision that conformational changes in the complex mediated by ATP hydrolysis in the cytoplasm activates CwIO-dependent cleavage of peptide cross-bridges between the glycan strands during growth (Fig. 8A). In the case of EnvC in *E. coli* and PcsB in *S. pneumoniae*, the coiled-coil domains of these proteins were found to specifically interact with the extracytoplasmic loop of FtsX, and this interaction is likely critical for the

regulation of these factors by the FtsEX complex. We were unable to detect a direct interaction between CwIO and this loop, but suspect this is because the interaction is augmented by another membrane-associated partner in the *B. subtilis* system resulting in a lower affinity between the isolated domains. Nevertheless, the most likely scenario is that CwIO is also controlled by FtsX via a mechanism analogous to the regulation of EnvC and PcsB (Fig. 8A). In support of this idea, an interaction between CwIO and FtsX has been observed by Errington and co-workers (Dominguez-Cuevas *et al.*, 2013).

FtsEX has now been implicated in the regulation of three different PG hydrolase families belonging to two different structural classes: EnvC with a LytM domain, and PcsB and CwIO with CHAP and NlpC/P60 domains respectively (Firczuk and Bochtler, 2007). Our results also indicate that in addition to controlling cell division in some organisms, FtsEX participates in the regulation of PG cleavage during the elongation phase of growth in *Bacillus* species. Interestingly, according to the prevailing views of the respective processes, the topology of the PG cleavage events required for daughter cell separation and for the insertion of new glycan strands into the stress-bearing layer of PG in Gram-positive bacteria are remarkably similar (Fig. 8B and C). In both cases, the PG is thought to be multilayered, and the PG hydrolases are tasked with cleaving membrane-distal PG layers while leaving the membrane-proximal material intact. Given the similarity of the cleavage events and the fact that FtsEX can interface with a variety of PG

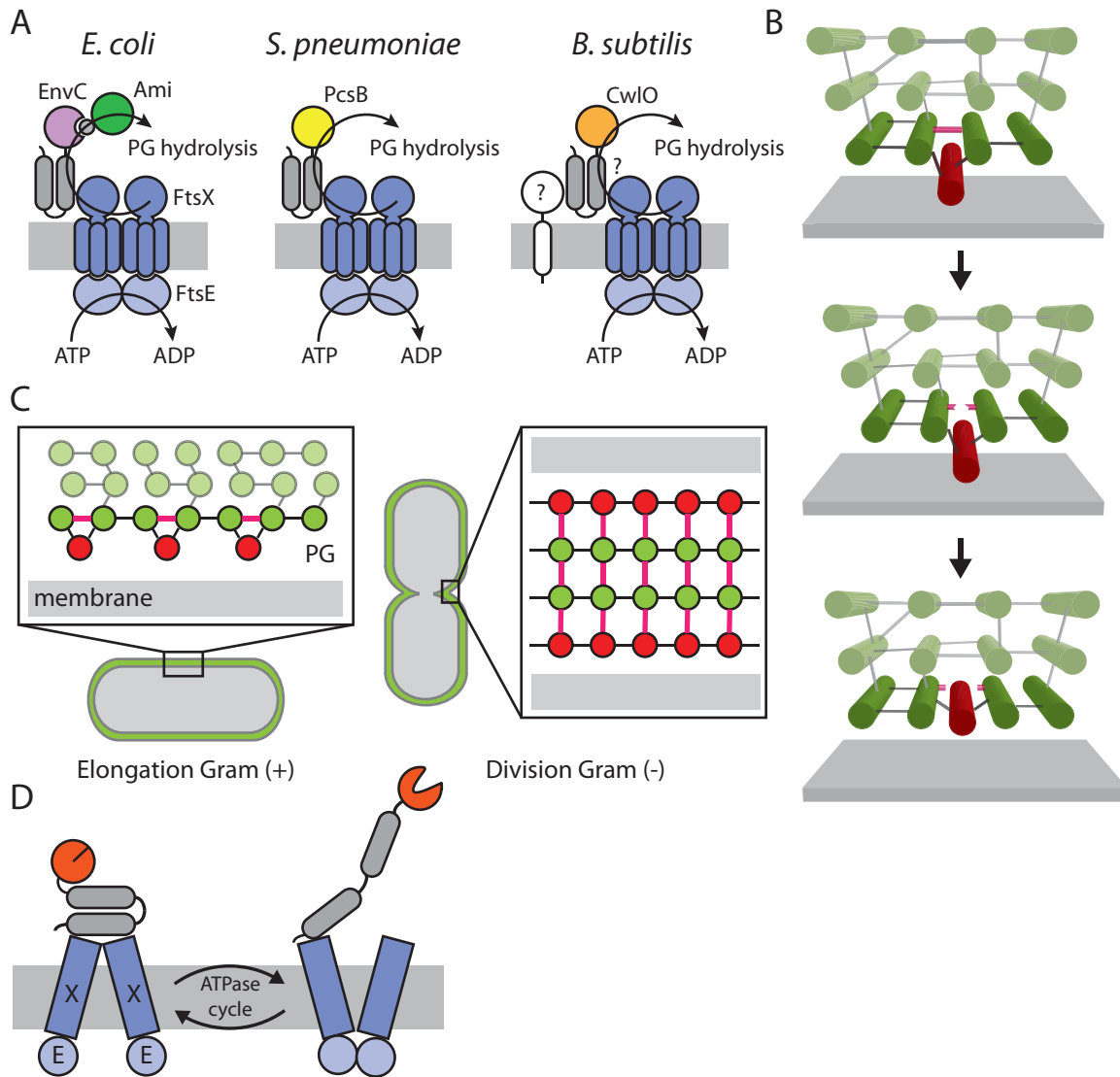


**Fig. 8.** FtsEX is a flexible regulatory module.

**A.** Schematic diagram of FtsEX and its regulatory pathway in *E. coli*, *S. pneumoniae*, and *B. subtilis*. FtsE-dependent ATP hydrolysis in the cytoplasm triggers PG hydrolysis outside the cell. A hypothetical membrane anchored protein (white) that holds CwlO at the cell surface is included. The hypothesized interaction between CwlO and FtsX is indicated with a question mark.

**B.** Schematic 3-dimensional diagrams of cell wall biogenesis during growth in *B. subtilis*. The PG layer adjacent to the cell membrane is shown in dark green while the other layers are represented schematically in light green. A newly synthesized glycan strand that has been cross-linked to adjacent older strands is shown in red. Peptide cross-link cleavage is shown (in hot pink) followed by incorporation of the new strand into the existing layer.

**C.** Comparison of multilayer PG during elongation in Gram (+) bacteria (left) and division in Gram (-) bacteria (right). Colour scheme for glycan strands and peptide cross-links is the same as in (B).

**D.** Proposed model for the regulation of diverse PG hydrolases by the FtsEX complex. Conformational changes in FtsEX (blue) mediated by ATP hydrolysis triggers a physical repositioning of the coiled-coil containing hydrolase such that it extends through the membrane proximal PG layer (not shown) to process membrane-distal cross-links.

hydrolases or PG hydrolase-like effectors, the regulatory mechanism employed is likely to be relatively simple and flexible. We favour a model in which the long, coiled-coil domains anchor the different PG hydrolases to the cell surface at least in part via the interaction with FtsX and position them such that the PG layers are just out of reach. We envision that conformational changes in FtsEX medi-

ated by ATP hydrolysis triggers a physical repositioning of the enzymes such that they extend through the membrane proximal PG layer to process membrane-distal cross-links (Fig. 8D). If this model is correct, virtually any PG hydrolase domain appended to the appropriate coiled-coil could be controlled by this conserved regulatory module. However, an additional layer of regulatory control that might exist

on top of this simple model is an autoinhibitory role for the coiled-coil domain in regulating the activity of the C-terminal PG hydrolase or PG hydrolase-like effector (Yang *et al.*, 2011).

#### *Co-ordinating PG hydrolysis by CwIO with the synthetic machinery*

In *E. coli* and *S. pneumoniae*, the FtsEX complex is linked to the divisome and therefore could be sensing the constriction of the FtsZ (tubulin) cytokinetic ring and/or the status of its PG synthases in order to transduce this information to PG hydrolases at the cell surface (Yang *et al.*, 2011). We suspect that because of its role in cell elongation, FtsEX in *B. subtilis* is similarly interfacing with the actin-directed cell elongation machinery to co-ordinate PG hydrolysis by CwIO with the polymerization status of the MreB/Mbl/MreBH polymers or the activity of its associated PG synthetic enzymes. In support of this model, Errington and co-workers have recently shown that FtsEX can be chemically cross-linked to complexes that contain the three MreB isoforms *in vivo* (Kawai *et al.*, 2011). Intriguingly, an FtsX–GFP fusion was also previously shown to localize as foci in the peripheral membrane in a pattern reminiscent of other components the PG synthetic machinery (Garti-Levi *et al.*, 2008). However, this fusion does was shown to be non-functional (Garti-Levi *et al.*, 2008) and in our hands did not support growth in the absence of LytE. Our inability to generate functional fluorescent fusions to FtsE, FtsX, or CwIO has prevented us from monitoring their dynamics to assess whether they associate with the elongation machinery and move with it. Thus, improved tools will be needed to assess the precise spatiotemporal connections between the FtsEX–CwIO system and the PG elongation machinery.

#### *PG synthesis during elongation in E. coli and B. subtilis*

Recent work in *E. coli* has defined three functionally redundant endopeptidases required for cell wall elongation (Singh *et al.*, 2012). In support of the idea that cell wall synthesis is intimately coupled to PG processing in *E. coli*, depletion of these PG hydrolases results in a significant reduction in cell wall synthesis prior to lysis as assessed by monitoring the incorporation of radio-labelled meso-diaminopimelic acid (mDAP) into the sacculus. These observations are consistent with a model in which cleavage of the peptide cross-bridges is necessary for continued synthesis and the insertion of new glycan strands between existing ones in the meshwork. Thus, the hydrolases in this case can be considered to function as ‘space-makers’ working in advance of a synthetic system travelling in their wake (Burman and Park, 1984). Such a model is readily

compatible with the thin, largely single-layered PG matrix found in *E. coli* and other Gram-negative bacteria. The situation is likely to be very different in Gram-positive bacteria like *B. subtilis*, which have to expand a thick multilayered PG sacculus via an inside-to-outside growth mechanism (Koch and Doyle, 1985). This mode of growth is thought to involve the synthesis of new PG material underneath the stress-bearing layers before subsequent cleavage events promote the movement of this material into the stress bearing structure (Fig. 8B) (Koch *et al.*, 1981). Consistent with this make-before-break mode of synthesis, our data indicate that the cell wall synthetic machinery continues to move circumferentially until lysis upon inactivation of the essential elongation hydrolases CwIO and LytE.

Interestingly, and consistent with the differences between the likely modes of growth between Gram-negative and Gram-positive PG, the PG hydrolases required for elongation in the different organisms have distinct cleavage specificities with important implications for the incorporation of new material. In *E. coli*, the elongation enzymes are DD-endopeptidases that cleave the same bond that forms the cross-links between peptides on adjacent strands (between the meso-diaminopimelic acid of one peptide and the D-alanine of the other) (Singh *et al.*, 2012). In cleaving this bond, both stem peptides retain the ability to serve as acceptors for cross-links with newly synthesized strands. Thus, enzymes with this specificity can easily act in advance of synthesis. By contrast, CwIO and LytE are DL-endopeptidases that cleave the bond between  $\gamma$ -D-glutamate and diaminopimelic acid within the stem peptide (Ishikawa *et al.*, 1998; Yamaguchi *et al.*, 2004). Because mDAP is lost from the peptide following such a cleavage, it cannot participate in cross-links with new material. Thus, the *B. subtilis* elongation endopeptidases are more suited for PG cleavage events that facilitate incorporation of previously cross-linked material into a pre-existing stress bearing layer (Fig. 8B).

#### *Regulation of LytE and other PG hydrolases*

Less is known about how the second elongation DL-endopeptidase, LytE, is regulated. Previous work has suggested that the MreB isoform MreBH directs LytE to sites of new cell wall synthesis (Carballido-Lopez *et al.*, 2006). Intriguingly, LytE and MreBH are both under  $\sigma^l$  control (Tseng and Shaw, 2008; Tseng *et al.*, 2011). If MreBH is indeed required for LytE activity then MreBH mutants would be predicted to display synthetic interactions with mutants in CwIO and FtsEX. However, we did not observe a significant impact on cell growth when either of these proteins was depleted in cells lacking MreBH (Fig. 4A and B). Accordingly, if MreBH and LytE are indeed

in a common regulatory pathway, other MreB isoforms are likely able to at least partially compensate for the absence of MreBH.

In addition to cell elongation, LytE has been implicated in PG degradation during cell division where it promotes cell separation (Ishikawa *et al.*, 1998). Mutants with LytE defects display a mild chaining phenotype, and LytE inactivation strongly enhances the cell separation phenotype of mutants defective in LytF (Ohnishi *et al.*, 1999). Cleavage of PG during cell separation in *B. subtilis* has markedly different spatial characteristics from hydrolysis during cell wall elongation. With its thick PG matrix, the layers to be cleaved for separation are likely to be several layers away from the cell membrane and the peptide cross-links are unlikely to be load bearing and consequently not under stress. This arrangement raises the possibility that the principal function of LytE in cell wall elongation is breaking bonds at a distance from the membrane to shed the outer layers that are no longer load bearing. In the context of this model, LytE could compensate for CwlO mutants by cleaving load-bearing cross-links (albeit inefficiently) in transit through the meshwork. Although this activity is sufficient to support elongation of the PG, it is likely not ideal and could account for the shorter and wider cell morphology associated with cells lacking CwlO and/or FtsEX. Irrespective of the precise substrate of LytE, the mechanism by which its PG hydrolytic activity is controlled remains to be elucidated. The range of different PG hydrolases typically encoded by bacterial genomes suggests that FtsEX is but one of many possible PG hydrolase regulatory systems. We anticipate that these systems will prove to be just as diverse and varied as the enzymes they control.

## Experimental procedures

### General methods

All *B. subtilis* strains were derived from the prototrophic strain PY79 (Youngman *et al.*, 1983). Unless otherwise indicated, cells were grown in LB or CH medium at 37°C. Sporulation was induced by resuspension according to the method of Sterlini-Mandelstam (Harwood and Cutting, 1990).  $\beta$ -Galactosidase assays were performed as described previously (Rudner *et al.*, 1999). Insertion-deletion mutations were generated by isothermal assembly (Gibson, 2011) of PCR products followed by direct transformation into *B. subtilis*. Protoplasts were generated at room temperature in hypertonic medium (0.5 M sucrose, 20 mM maleic acid pH 6.5, and 20 mM MgCl<sub>2</sub>) with 0.5 mg ml<sup>-1</sup> lysozyme. Protoplasts were disrupted with Triton X-100 at a final concentration of 0.1%. Proteinase K (final concentration 50  $\mu$ g ml<sup>-1</sup>) was used to determine protease accessibility of CwlO. Tables of strains, plasmids and oligonucleotide primers and a description of strain and plasmid construction can be found online as supplementary data (Tables S1, S2 and S3, and Text S1).

### Immunoblot analysis

Whole cell lysates from vegetatively growing cells were prepared as described (Doan and Rudner, 2007). Samples were heated for 10 min at 55°C prior to loading. Equivalent loading was based on OD<sub>600</sub> at the time of harvest. Proteins were separated by SDS-PAGE on 12.5% polyacrylamide gels, electroblotted onto Immobilon-P membranes (Millipore) and blocked in 5% non-fat milk in phosphate-buffered saline (PBS)-0.5% Tween-20. The blocked membranes were probed with anti-FtsE (1:10 000), anti-CwlO (1:10 000), anti-FtsX (1:10 000), anti-ClpX (1:5000) (Haeusser *et al.*, 2009) and anti-Spo0J (1:5000) (Lin and Grossman, 1998) diluted into 3% BSA in 1 $\times$  PBS-0.05% Tween-20. Primary antibodies were detected using horseradish peroxidase-conjugated goat anti-rabbit IgG (Bio-Rad) and the Super Signal chemiluminescence reagent as described by the manufacturer (Pierce).

### Protein purification and antibody production

Recombinant proteins were expressed in *E. coli* strain BL21 (DE3). Strains were grown in LB medium supplemented with 100  $\mu$ g ml<sup>-1</sup> ampicillin at 37°C and protein expression was induced by the addition of IPTG to a final concentration of 0.5 mM. After 3 h of induction, cultures were subjected to centrifugation at 10 000 *g* for 10 min. Cell pellets were resuspended in 100 mM Tris pH 7.5, 500 mM NaCl, 5 mM imidazole, 2 mM  $\beta$ -mercaptoethanol and Complete EDTA-free protease inhibitor (Roche). Cell suspensions were passed through a French press. Cell lysates were clarified by centrifugation at 10 000 *g* for 10 min at 4°C. Clarified lysates were injected onto 1 ml HisTrap FF columns (GE Healthcare) using an AKTA explorer 10 (GE Healthcare). The columns were washed with 10 ml Buffer A (100 mM Tris pH 7.5, 500 mM NaCl, 5 mM imidazole, and 2 mM  $\beta$ -mercaptoethanol). His6 or His6-SUMO fusion proteins were eluted with a 20 ml linear gradient (from 0% to 100%) of Buffer B (100 mM Tris pH 7.5, 500 mM NaCl, 500 mM imidazole, and 2 mM  $\beta$ -mercaptoethanol). Elution fractions were pooled (about 5 ml) and dialysed twice in 1 l 50 mM Tris pH 8.0, 150 mM NaCl, 2 mM  $\beta$ -mercaptoethanol, 10% glycerol at 4°C. Dialysed fractions containing His6-SUMO fusions proteins were incubated with His6-Ulp1 protease overnight on ice. Reactions were injected onto HisTrap FF columns and flow through fractions containing untagged proteins were collected and used to generate rabbit polyclonal antibodies (Covance).

### Fluorescence microscopy

Fluorescence microscopy was performed using a Nikon Ti microscope equipped with a plan apochromat 100 $\times$  1.4 NA phase contrast objective and a CoolSnapHQ digital camera (Photometrics). Images were acquired using Nikon Elements software. Membranes were stained with TMA-DPH (Molecular Probes). Image analysis and quantification were performed using MicrobeTracker (Sliuarenko *et al.*, 2011). Images were adjusted and cropped using Metamorph software. Final figure preparation was performed in Adobe Illustrator.

For snapshot imaging, cells were immobilized on 2% agarose pads containing growth medium. For time-lapse

imaging, cells were imaged on a glass bottom dish (WillCo). Exponentially growing cells were concentrated by centrifugation at 5000 r.p.m. for 2 min. 2 µl of the cell pellet was spotted onto the dish and a 2% agarose pad containing growth medium was then laid on top of the bacteria. Cells were imaged in a stage top incubator (Bioscience Tools) with controlled humidity and temperature. The upper face of the pad was fully exposed, allowing adequate oxygen for growth. The objective was maintained at the same temperature as the incubator using an objective heater (Biotechs). Images were acquired every 5 or 10 s as specified, using neutral density filters (ND4) to reduce photobleaching and phototoxicity.

## Acknowledgements

We thank members of the Rudner and Bernhardt labs, especially Tsuyoshi Uehara, for advice and encouragement, Eammon Riley for plasmid construction and two-hybrid analysis, Nick Peters and Chris Rodrigues for help with fluorescence imaging, and Alex Meeske for help with double mutant analysis. We thank Jeff Errington and co-workers for communicating results prior to publication. Support for this work comes from the National Institute of Health Grant GM086466 (D. Z. R.) and AI083365-01 (T. G. B.).

## References

- Arends, S.J., Kustusch, R.J., and Weiss, D.S. (2009) ATP-binding site lesions in FtsE impair cell division. *J Bacteriol* **191**: 3772–3784.
- Bateman, A., and Rawlings, N.D. (2003) The CHAP domain: a large family of amidases including GSP amidase and peptidoglycan hydrolases. *Trends Biochem Sci* **28**: 234–237.
- Beeby, M., Gumbart, J.C., Roux, B., and Jensen, G.J. (2013) Architecture and assembly of the Gram-positive cell wall. *Mol Microbiol* **88**: 664–672.
- Bisicchia, P., Noone, D., Lioliou, E., Howell, A., Quigley, S., Jensen, T., et al. (2007) The essential YycFG two-component system controls cell wall metabolism in *Bacillus subtilis*. *Mol Microbiol* **65**: 180–200.
- Buist, G., Steen, A., Kok, J., and Kuipers, O. (2008) LysM, a widely distributed protein motif for binding to (peptid)glycans. *Mol Microbiol* **68**: 838–847.
- Burdett, I.D., and Murray, R.G. (1974a) Electron microscope study of septum formation in *Escherichia coli* strains B and B-r during synchronous growth. *J Bacteriol* **119**: 1039–1056.
- Burdett, I.D., and Murray, R.G. (1974b) Septum formation in *Escherichia coli*: characterization of septal structure and the effects of antibiotics on cell division. *J Bacteriol* **119**: 303–324.
- Burman, L.G., and Park, J.T. (1984) Molecular model for elongation of the murein sacculus of *Escherichia coli*. *Proc Natl Acad Sci USA* **81**: 1844–1848.
- Carballido-Lopez, R., Formstone, A., Li, Y., Ehrlich, S.D., Noirot, P., and Errington, J. (2006) Actin homolog MreBH governs cell morphogenesis by localization of the cell wall hydrolase LytE. *Dev Cell* **11**: 399–409.
- Crawford, M.A., Lowe, D.E., Fisher, D.J., Stibitz, S., Plaut, R.D., Beaber, J.W., et al. (2011) Identification of the bacterial protein FtsX as a unique target of chemokine-mediated antimicrobial activity against *Bacillus anthracis*. *Proc Natl Acad Sci USA* **108**: 17159–17164.
- Doan, T., and Rudner, D.Z. (2007) Perturbations to engulfment trigger a degradative response that prevents cell-cell signalling during sporulation in *Bacillus subtilis*. *Mol Microbiol* **64**: 500–511.
- Dominguez-Cuevas, P., Porcelli, I., Daniel, R.A., and Errington, J. (2013) Differentiated roles for MreB actin isoforms and autolytic enzymes in bacterial morphogenesis. *Mol Microbiol* **89**: 1084–1098.
- Firczuk, M., and Bochtler, M. (2007) Folds and activities of peptidoglycan amidases. *FEMS Microbiol Rev* **31**: 676–691.
- Gan, L., Chen, S., and Jensen, G.J. (2008) Molecular organization of Gram-negative peptidoglycan. *Proc Natl Acad Sci USA* **105**: 18953–18957.
- Garner, E.C., Bernard, R., Wang, W., Zhuang, X., Rudner, D.Z., and Mitchison, T. (2011) Coupled, circumferential motions of the cell wall synthesis machinery and MreB filaments in *B. subtilis*. *Science* **333**: 222–225.
- Garti-Levi, S., Hazan, R., Kain, J., Fujita, M., and Ben-Yehuda, S. (2008) The FtsEX ABC transporter directs cellular differentiation in *Bacillus subtilis*. *Mol Microbiol* **69**: 1018–1028.
- Gibson, D.G. (2011) Enzymatic assembly of overlapping DNA fragments. *Methods Enzymol* **498**: 349–361.
- Haeusser, D.P., Lee, A.H., Weart, R.B., and Levin, P.A. (2009) ClpX inhibits FtsZ assembly in a manner that does not require its ATP hydrolysis-dependent chaperone activity. *J Bacteriol* **191**: 1986–1991.
- Harwood, C.R., and Cutting, S.M. (1990) *Molecular Biological Methods for Bacillus*. New York: Wiley.
- Hashimoto, M., Ooiwa, S., and Sekiguchi, J. (2012) Synthetic lethality of the *lytE cwI* genotype in *Bacillus subtilis* is caused by lack of D,L-endopeptidase activity at the lateral cell wall. *J Bacteriol* **194**: 796–803.
- Heidrich, C., Ursinus, A., Berger, J., Schwarz, H., and Holtje, J.V. (2002) Effects of multiple deletions of murein hydrolases on viability, septum cleavage, and sensitivity to large toxic molecules in *Escherichia coli*. *J Bacteriol* **184**: 6093–6099.
- Higgins, C.F. (1992) ABC transporters: from microorganisms to man. *Annu Rev Cell Biol* **8**: 67–113.
- Ishikawa, S., Hara, Y., Ohnishi, R., and Sekiguchi, J. (1998) Regulation of a new cell wall hydrolase gene, *cwI*, which affects cell separation in *Bacillus subtilis*. *J Bacteriol* **180**: 2549–2555.
- Jones, L.J., Carballido-Lopez, R., and Errington, J. (2001) Control of cell shape in bacteria: helical, actin-like filaments in *Bacillus subtilis*. *Cell* **104**: 913–922.
- Kawai, Y., Marles-Wright, J., Cleverley, R.M., Emmins, R., Ishikawa, S., Kuwano, M., et al. (2011) A widespread family of bacterial cell wall assembly proteins. *EMBO J* **30**: 4931–4941.
- Koch, A.L., and Doyle, R.J. (1985) Inside-to-outside growth and turnover of the wall of gram-positive rods. *J Theor Biol* **117**: 137–157.
- Koch, A.L., Higgins, M.L., and Doyle, R.J. (1981) Surface tension-like forces determine bacterial shapes: *Streptococcus faecium*. *J Gen Microbiol* **123**: 151–161.

- Lin, D.C., and Grossman, A.D. (1998) Identification and characterization of a bacterial chromosome partitioning site. *Cell* **92**: 675–685.
- Margot, P., Wahlen, M., Gholamhoseinian, A., Piggot, P., and Karamata, D. (1998) The *lytE* gene of *Bacillus subtilis* 168 encodes a cell wall hydrolase. *J Bacteriol* **180**: 749–752.
- Ohnishi, R., Ishikawa, S., and Sekiguchi, J. (1999) Peptidoglycan hydrolase *LytF* plays a role in cell separation with CwlF during vegetative growth of *Bacillus subtilis*. *J Bacteriol* **181**: 3178–3184.
- Olijhoek, A.J., Klencke, S., Pas, E., Nanninga, N., and Schwarz, U. (1982) Volume growth, murein synthesis, and murein cross-linkage during the division cycle of *Escherichia coli* PA3092. *J Bacteriol* **152**: 1248–1254.
- Priyadarshini, R., de Pedro, M.A., and Young, K.D. (2007) Role of peptidoglycan amidases in the development and morphology of the division septum in *Escherichia coli*. *J Bacteriol* **189**: 5334–5347.
- Rees, D.C., Johnson, E., and Lewinson, O. (2009) ABC transporters: the power to change. *Nat Rev Mol Cell Biol* **10**: 218–227.
- Rudner, D.Z., Fawcett, P., and Losick, R. (1999) A family of membrane-embedded metalloproteases involved in regulated proteolysis of membrane-associated transcription factors. *Proc Natl Acad Sci USA* **96**: 14765–14770.
- Salzberg, L.I., Powell, L., Hokamp, K., Botella, E., Noone, D., and Devine, K.M. (2013) The WalRK (YycFG) and sigma(I) RsgI regulators cooperate to control CwlO and *LytE* expression in exponentially growing and stressed *Bacillus subtilis* cells. *Mol Microbiol* **87**: 180–195.
- Sham, L.T., Barendt, S.M., Kopecky, K.E., and Winkler, M.E. (2011) Essential PcsB putative peptidoglycan hydrolase interacts with the essential FtsX<sub>Spn</sub> cell division protein in *Streptococcus pneumoniae* D39. *Proc Natl Acad Sci USA* **108**: E1061–E1069.
- Singh, S.K., SaiSree, L., Amrutha, R.N., and Reddy, M. (2012) Three redundant murein endopeptidases catalyse an essential cleavage step in peptidoglycan synthesis of *Escherichia coli* K12. *Mol Microbiol* **86**: 1036–1051.
- Sliusarenko, O., Heinritz, J., Emonet, T., and Jacobs-Wagner, C. (2011) High-throughput, subpixel precision analysis of bacterial morphogenesis and intracellular spatio-temporal dynamics. *Mol Microbiol* **80**: 612–627.
- Tseng, C.L., and Shaw, G.C. (2008) Genetic evidence for the actin homolog gene *mreBH* and the bacitracin resistance gene *bcrC* as targets of the alternative sigma factor SigI of *Bacillus subtilis*. *J Bacteriol* **190**: 1561–1567.
- Tseng, C.L., Chen, J.T., Lin, J.H., Huang, W.Z., and Shaw, G.C. (2011) Genetic evidence for involvement of the alternative sigma factor SigI in controlling expression of the cell wall hydrolase gene *lytE* and contribution of *LytE* to heat survival of *Bacillus subtilis*. *Arch Microbiol* **193**: 677–685.
- Uehara, T., Parzych, K.R., Dinh, T., and Bernhardt, T.G. (2010) Daughter cell separation is controlled by cytokinetic ring-activated cell wall hydrolysis. *EMBO J* **29**: 1412–1422.
- Van De Putte, P., Van, D., and Roersch, A. (1964) The selection of mutants of *Escherichia coli* with impaired cell division at elevated temperature. *Mutat Res* **106**: 121–128.
- Vollmer, W., Joris, B., Charlier, P., and Foster, S. (2008) Bacterial peptidoglycan (murein) hydrolases. *FEMS Microbiol Rev* **32**: 259–286.
- Weidel, W., and Pelzer, H. (1964) Bagshaped macromolecules – a new outlook on bacterial cell walls. *Adv Enzymol Relat Areas Mol Biol* **26**: 193–232.
- Yamaguchi, H., Furuhashi, K., Fukushima, T., Yamamoto, H., and Sekiguchi, J. (2004) Characterization of a new *Bacillus subtilis* peptidoglycan hydrolase gene, *yvcE* (named *cwlO*), and the enzymatic properties of its encoded protein. *J Biosci Bioeng* **98**: 174–181.
- Yang, D.C., Peters, N.T., Parzych, K.R., Uehara, T., Markovski, M., and Bernhardt, T.G. (2011) An ATP-binding cassette transporter-like complex governs cell-wall hydrolysis at the bacterial cytokinetic ring. *Proc Natl Acad Sci USA* **108**: E1052–E1060.
- Youngman, P.J., Perkins, J.B., and Losick, R. (1983) Genetic transposition and insertional mutagenesis in *Bacillus subtilis* with *Streptococcus faecalis* transposon Tn917. *Proc Natl Acad Sci USA* **80**: 2305–2309.

## Supporting information

Additional supporting information may be found in the online version of this article at the publisher's web-site.